Effects of Draw Bending Conditions of Tube on Deformation of the Bent Tube during the Subsequent Hydroforming Process

Katsushi Ishigaki*[1], Naoyoshi Sakaguchi[1] , Naoto Kaneda[1] and Masayasu Kojima[1]
[1]Yamamoto Hydraulic Machinery Works Co.,LTD

Abstract: This paper describes a sequential FEM simulation of draw bending of tube and hydroforming of the bent tube. The effects of draw bending conditions such as mandrel inserted the tube and axial compression applied to the end of the tube on the thinning behavior during the hydroforming are made clear. Minimizing the amount of flattening of the bend by using a multiple ball mandrel is effective to decrease thinnings of the outside and the side walls of the bend during the hydroforming. Increasing the axial compression of the tube during the draw bending is effective to increase the thicknesses of the outside and the side walls of the bend after the hydroforming.

Keywords: Draw bending, hydroforming, ball mandrel, axial compression, flattening.

1. Introduction

Structural parts with hollow section for auto-body manufactured by tube hydroforming process have two or more bends along the axis. Prior to the hydroforming of these parts, a straight tube blank for each part is bent on a draw bending machine to approximately the final shape of the part. During the bending operation, non-uniform circumferential distributions of wall thickness and work-hardening are formed in the bend, therefore, expansion ratio of the bend in the subsequent hydroforming process should be limited to prevent localized thinning or bursting. In this paper, a sequential FEM simulation of draw bending and hydroforming is performed for the purpose of making clear the suitable draw bending conditions to decrease the thinning of the bend during the hydroforming and to increase the thickness of the bend after the hydroforming.

2. Simulation model (Solver=LS-DYNA)

2.1 Tube blank

Steel tube with diameter of 60.5mm, wall thickness of 2mm, and length of 418mm is modelled by shell elements. The periphery of the tube is composed of 120 elements with axial edge length of 2mm. Stress-strain relationship of the tube is shown in Fig.1. Yield point σy, Young's modulus E, slope of the linear work-hardening Et, and Poisson's ratio ν are listed in Table 1.

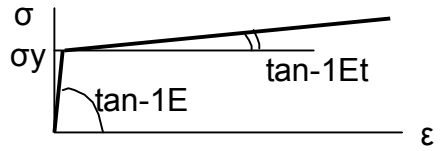

Figure 1 Stress-strain relationship of tube

Table 1 Mechanical properties of tube

Yield point σy	354 [MPa]
Young's modulus E	206 [GPa]
Slope of linear work-hardening Et	1.26 [GPa]
Poisson's ratio ν	0.3

2.2 Draw bending

The tube blank is bent at an angle of 90° with a centerline radius of 120mm as shown in Fig.2. Fig.2 (a) shows tooling before starting the bending operation. Bending tools are bending form, clamp die, movable pressure die, wiper die, and flexible ball mandrel. The surfaces of the bending tools are modeled by rigid shell elements. The wiper die is fixed to the main body of the bender with a heel angle of 0.5° . Nodes at the top of the tube are fixed with both the straight clamping section of the bending form and the mating clamp die. Table 2 shows coefficient of friction in the contact interfaces between the tube and the bending tools. In this simulation, four kinds of mandrel conditions are studied. They are 1-ball, 2-ball, 3-ball shown in Fig.3 and without mandrel. The ball mandrel consists of a shank and ball segments. The shank and the ball segments are connected with ball joints. The clearance between the tube and the ball mandrel is 0.5mm. The ball mandrel supported by a rod is positioned as shown in Fig.2. In this study, axial compressive stress fb applied to the end of the tube is considered as another bending condition by which the thickness of the bend after hydroforming will be controlled. The magnitude of fb is constant during the draw bending process.

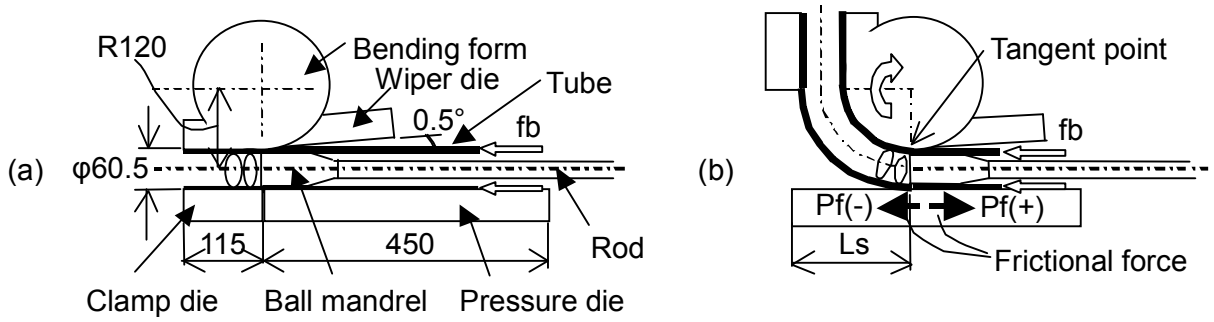

Figure 2 Simulation model of draw bending of tube

Table 2 Coefficient of friction during bending

Bending tools	Coefficient of friction
Bending form	0.1
Clamp die	0.5
Pressure die	0.2
Wiper die	0.1
Ball mandrel	0.1

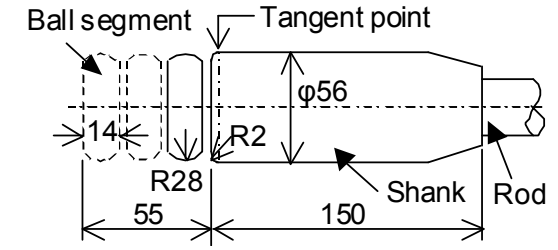

Figure 3 Ball mandrel(1-ball,2-ball,3-ball)

Fig.2 (b) shows the final state of the draw bending operation. In this simulation, the pressure die is moved with a constant velocity during the rotation of the bending form. Displacement of the pressure die (*Ls*) for the bending angle of 90° can be determined arbitrarily. In this study, the magnitude of the displacement of the pressure die is expressed by non-dimensional *γ* defined by Eq.1.

$$\gamma = Ls/(R\theta) \tag{1}$$

Where *R* is bending radius (=120mm), *θ* is bending angle in radian (=π/2). Depending on the magnitude of *γ*, velocity of the pressure die to the tube is varied, and consequently, the longitudinal frictional force *Pf* (see Fig.2 (b)) applied to the pressure die from the tube is varied. In the simulation, the direction of *Pf* is distinguished by the sign of plus or minus. Minus *Pf* is forward frictional force and plus *Pf* is backward frictional force. As the direction of the frictional force applied to the tube from the pressure die is reverse to the direction of *Pf*, minus *Pf* and plus *Pf* act as backward tension and forward compression for the tube respectively.

2.3 Hydroforming

Dimensions of the hydroformed workpiece are shown in Fig.4. The bent tube illustrated by dotted line is set in the hydroforming die and the bend of the bent tube is expanded to 1.1 times the diameter of the tube blank by increasing the internal pressure. The edge nodes in the bent tube are fixed to the hydroforming die to simulate the hydroforming without axial feeding. Coefficient of friction in the contact interface between the tube and the die is 0.1.

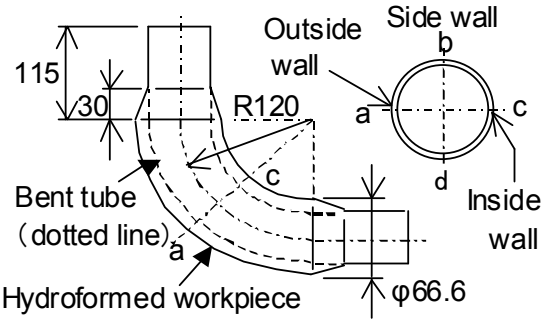

Figure 4 Dimensions of hydroformed workpiece

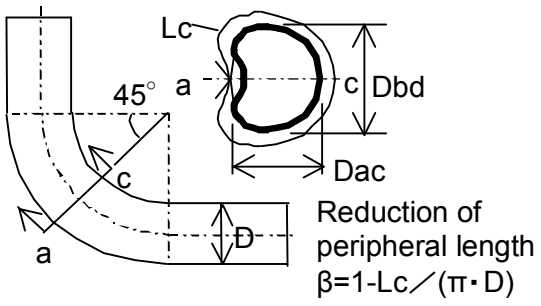

Figure 5 Dimensions of 45° cross section of bend

3. Simulation results on the effects of mandrel conditions

3.1 Flattening of the bend in draw bending

The role of the mandrel in the draw bending is reduction of the amount of flattening[1]. In this study the flatness of the bend is defined by Eq.2.

$$\alpha=(Dbd-Dac)/D \quad (2)$$

Where Dac and Dbd are diameters at 45° cross section shown in Fig.5, and D is diameter of the tube blank. Fig.6 (a) and (b) show the variations of *Pf* and flatness *α* with *γ* respectively. From Fig.6 (a) and (b), it is observed that *α* decreases with the change of the sign of *Pf* from minus to plus, and the variations of *α* with *Pf* are reduced with increasing the number of the ball segment. In this study, the effects of the mandrel condition on *α* are evaluated at critical $\gamma(=\gamma_{cr})$ which makes *Pf* zero. Fig.7 shows variations of *α*, reduction of peripheral length *β*(see Fig.5), and shape of 45° cross section of the bend with mandrel conditions. In the case of bending without mandrel, concaved deflection is observed on the flattened outside wall. From Fig.7, it is clear that large *α* brings large *β*, and consequently, increases the actual expansion ratio during the subsequent hydroforming process.

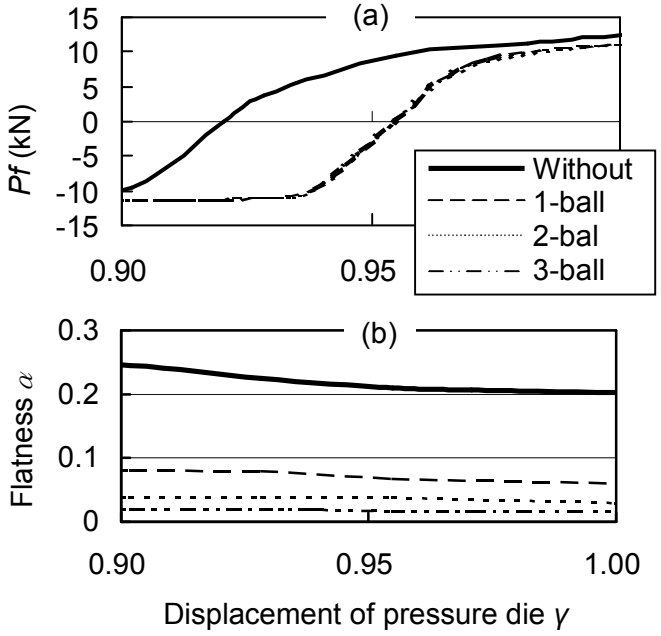

Figure 6 Variations of frictional force Pf and flatness α with γ (fb=0)

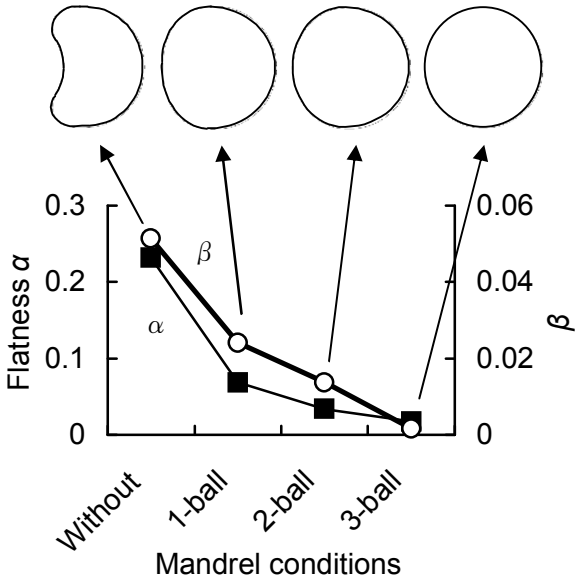

Figure 7 Variations of flatness and reduction of peripheral length β with mandrel conditions (fb=0, $\gamma=\gamma_{cr}$)

3.2 Expanding behavior of the bend during the hydroforming

Enlargement of the cross section of the bend is observed by measuring the clearance between the wall of the bend and the wall of the die cavity at 45° cross section. Fig.8 (a), (b), and (c) show variations of the clearance *δ* at the outside, the side, and inside walls respectively, with the increase of the internal pressure *p*. In Fig.8 (a), difference of the initial *δ* at *p*=0 among the mandrel conditions is due to the difference of *α* shown in Fig.7. The larger the initial *δ*, the faster the flattened outside wall is expanded out with increasing *p*. It seems that the outside, the side, and the inside walls contact with the mating wall of the die cavity at almost the same *p* for the mandrel conditions of 1-ball, and 3-ball. Fig.9 (a), (b), and (c) show variations of longitudinal strain *εl* on the outside, the side, and the inside walls at 45° cross section with increasing *p* for the condition of without mandrel, 1-ball, and 3-ball respectively. For all mandrel conditions, the change of *εl* during the hydroforming is plus at the outside wall, nearly zero at the side wall, and minus at the inside wall, as expected from the difference of the longitudinal curvature radius between the bent tube and the hydroformed tube shown in Fig.4. In the condition without mandrel shown in Fig.9 (a), increase of *εl* starts at low pressure (less than 20MPa) corresponding to the reduction of *δ* at the initial stage of increasing *p* shown in Fig.8 (a). Comparing Fig.9 (a), (b), and (c), it is observed that the increase of *εl* on the outside wall during hydroforming is reduced by using a multiple ball mandrel.

Fig.10 (a), (b), and (c) show variations of circumferential strain $\varepsilon\theta$ on the outside, the side, and the inside walls at 45° cross section with increasing p for the condition of without mandrel, 1-ball, and 3-ball respectively. It is observed that $\varepsilon\theta$ on the side wall starts to increase at less p than that on the outside and the inside walls, and that the increase of $\varepsilon\theta$ on the side wall is noticeably larger than that on the outside and the inside walls. It is considered that the phenomenon of increasing $\varepsilon\theta$ on the side wall is mainly due to the fact that the work-hardening during the draw bending of the side wall is noticeably less than that on the outside and the inside walls.

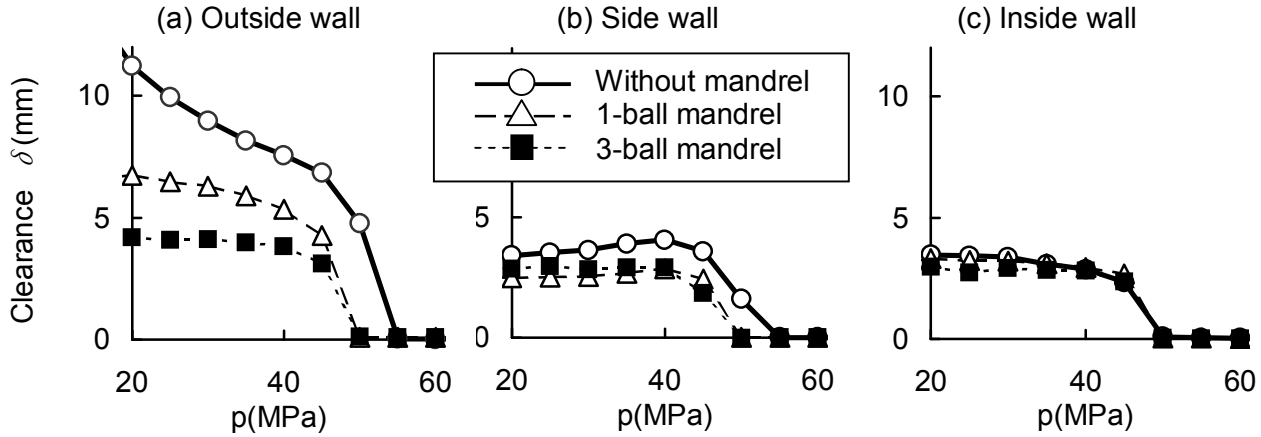

Figure 8 Variations of clearance between wall of die cavity and bent tube with increase of internal pressure (fb=0, $\gamma=\gamma_{cr}$)

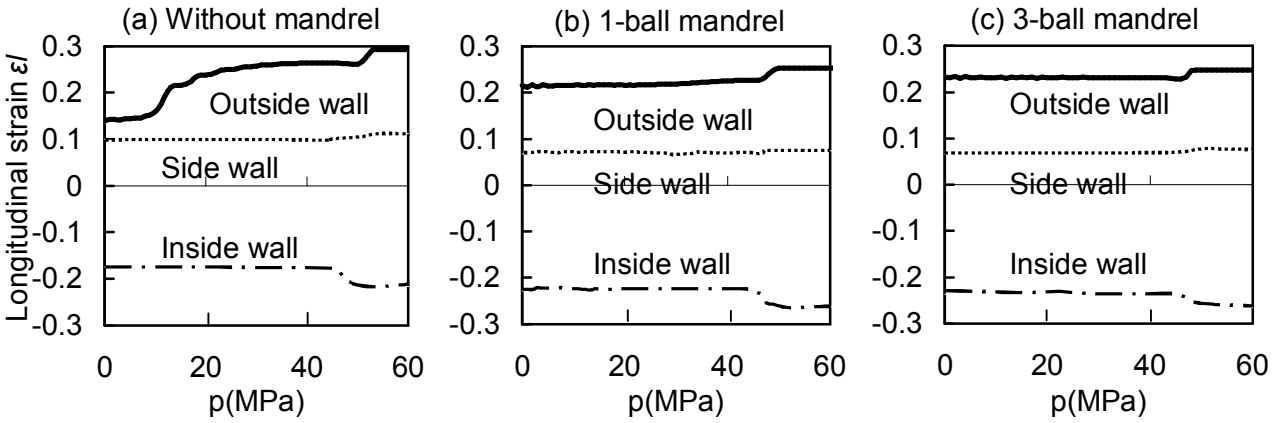

Figure 9 Variations of longitudinal strain at 45° cross section of bent tube with increase of internal pressure (fb=0, $\gamma=\gamma_{cr}$)

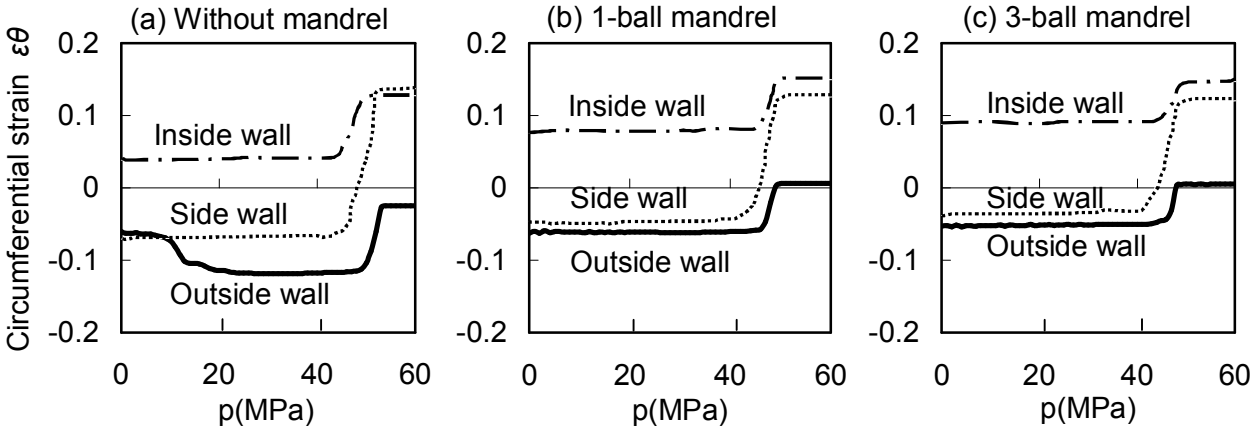

Figure 10 Variations of circumferential strain at 45° cross section of bent tube with increase of internal pressure (fb=0, $\gamma=\gamma_{cr}$)

In Fig.10, it is also observed that the increase of $\varepsilon\theta$ on the side wall is reduced by using a multiple ball mandrel. In the condition without mandrel shown in Fig.10 (a), it must be noticed that $\varepsilon\theta$ on the outside wall is reduced at low pressure (less than 20MPa). This means that the peripheral length of the bend, which is reduced largely during the bending without mandrel, is reduced again at the initial stage of the hydroforming. The reduction of the peripheral length of the bend due to the reduction of εθ on the outside wall increases the total expansion ratio during the hydroforming. Fig.11 (a), (b), and (c) show variations of the thickness strain at 45° cross section of the bent tube and the hydroformed tube with mandrel conditions on the outside, the side, and the inside walls respectively. In the case of the circular expansion by the hydroforming in this study, the most thinned area after the hydroforming is the outside wall for all mandrel conditions. From Fig.11 (a), it is noticed that the degree of thinning of the outside wall after the hydroforming is hardly affected by the mandrel conditions, while the thinning of the outside wall after bending increases by using a multiple ball mandrel. In other words, it can be said that the larger the amount of flattening in the draw bending, the larger the thinning of the outside wall during the hydroforming. Comparing the differences between the thickness strain after draw bending and that after hydroforming in Fig.11 (a), (b), and (c), it is clearly observed that the thinning during the hydroforming of the side wall is noticeably larger than that of the outside and inside walls. From Fig.11 (b), it is noticed that the thinning of the side wall during the hydroforming is reduced by using the multiple ball mandrel. The thinning of the inside wall during the hydroforming is small and is hardly affected by the mandrel conditions as shown in Fig.11 (c).

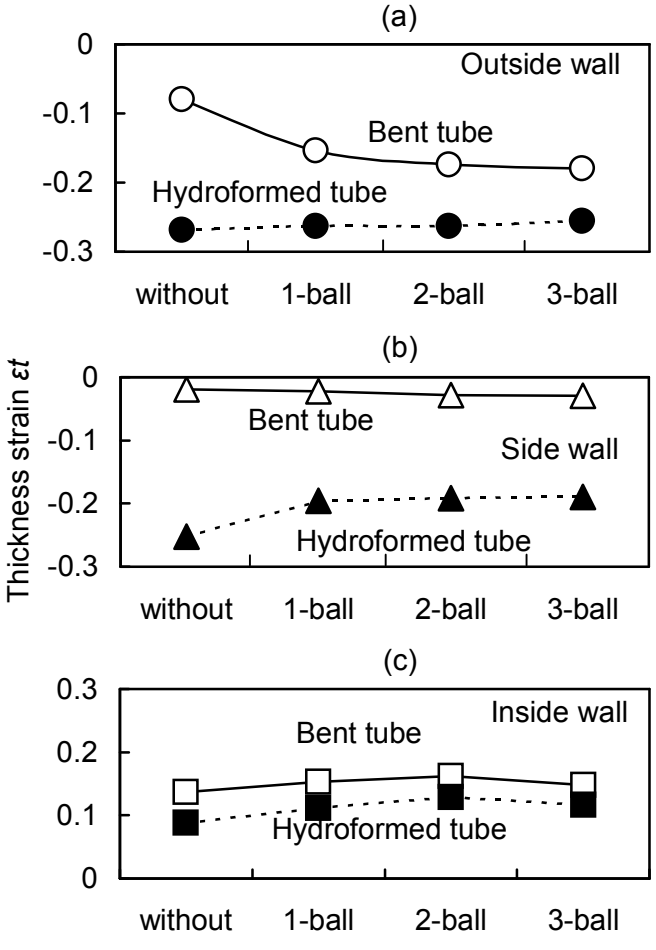

Figure 11 Variations of thickness strain at 45° cross section of bent tube and hydroformed tube with mandrel conditions in draw bending (fb=0, γ=γ_{cr})

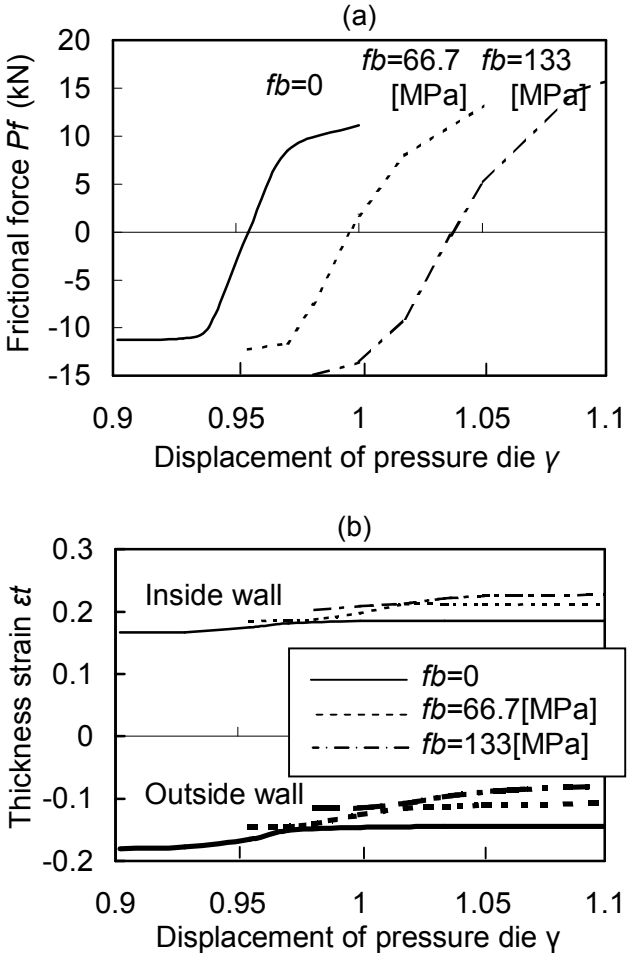

Figure 12 Effects of axial compressive stress fb on variations of frictional force Pf and thickness strain with γ (3-ball mandrel)

4. Simulation results on the effects of axial compression applied to the tube during bending

4.1 Thinning and thickening in draw bending

It is known that the compressive stress applied to the tube by using a booster decreases the thinning of the outside wall of the bend and increases the thickening of the inside wall of the bend [2]. Both the thinning and the thickening are also affected by the direction of the frictional force *Pf*. Fig.12 (a) and (b) show effects of the compressive stress (*fb*) on the variations of *Pf* and thickness strain of the bend respectively, with the non-dimensional displacement (γ) of the pressure die in the draw bending with 3-ball mandrel. In Fig.12 (a), it is clear that γ_{cr}, which makes *Pf* zero, increases with the increase of *fb*. And in Fig.12 (b), it is observed that the thinning of the outside wall is decreased and the thickening of the inside wall is increased by the change of the sign of *Pf* from minus to plus accompanied with the increase of γ. The effects of *fb* on the thinning and the thickening of the bend should be evaluated by the thickness strain obtained at the condition of γ_{cr} for each value of *fb*.

4.2 Thickness strain of the bend after hydroforming

Fig.13 (a), (b), and (c) show variations of thickness strain at 45° cross section of the bent tube and the hydroformed tube with *fb* on the outside wall, the side wall, and the inside wall respectively. Increase of *fb* is effective to increase the thickness of the outside wall and that of the side wall after the hydroforming. Differences of the thickness strain between the bent tube and the hydroformed tube on the outside, the side, and the inside walls are hardly affected by the magnitude of *fb*.

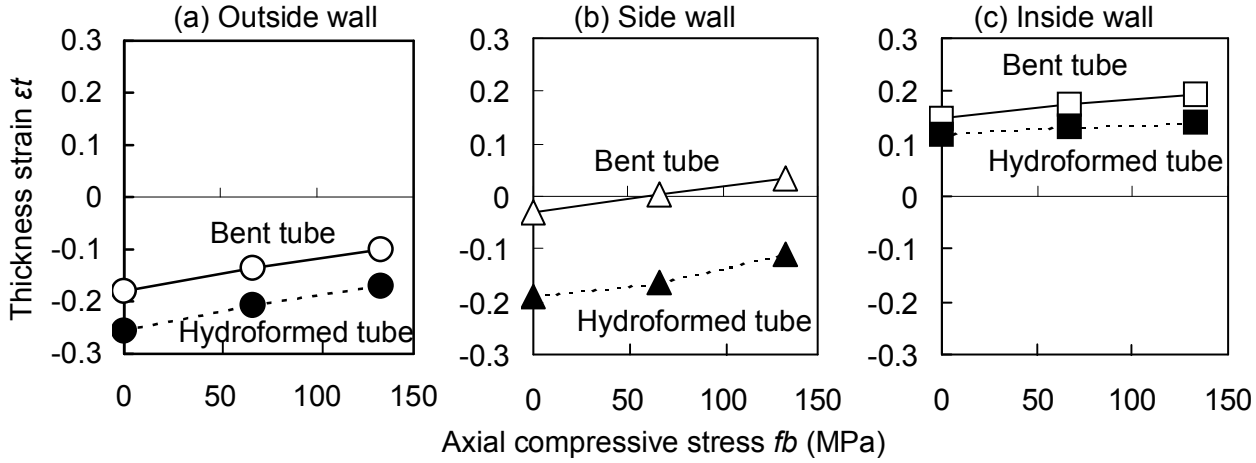

Figure 13 Variations of thickness strain at 45° cross section of the bent tube and the hydroformed tube with axial compressive stress at tube end in draw bending(3-ball mandrel, $\gamma=\gamma_{cr}$)

5. SUMMARY

Effects of the mandrel conditions and the compressive stress applied to the end of tube in the draw bending on the thinning behavior of the bend during the subsequent hydroforming are investigated by the sequential FEM simulation.

(1) The most thinned area after hydroforming is the outside wall and the most thinned area during hydroforming is the side wall for all mandrel conditions. Minimizing the amount of flattening of the bend by using a multiple ball mandrel is effective to decrease thinnings of the outside and the side walls during the hydroforming.

(2) Increasing the axial compression applied to the end of the tube during the draw bending is effective to increase the thicknesses of the outside and the side walls of the bend after the hydroforming.

REFERENCES

[1] R.J.Kervick, R.K.Springborn, 1966, “Cold bending and forming tube and other sections”, ASTME

[2] D.Park, Y.Kim, 2005, Effect analysis of bending process on hydroforming, “Proceedings of TUBEHYDRO2005“, PP.18-22